



HAL
open science

Matching of fundamental modes at a junction of a cylinder and a truncated cone; application to the calculation of radiation impedances

Jean Kergomard, Antoine Lefebvre, Gary Scavone

► To cite this version:

Jean Kergomard, Antoine Lefebvre, Gary Scavone. Matching of fundamental modes at a junction of a cylinder and a truncated cone; application to the calculation of radiation impedances. 2015. hal-01134302v1

HAL Id: hal-01134302

<https://hal.science/hal-01134302v1>

Preprint submitted on 23 Mar 2015 (v1), last revised 28 Apr 2016 (v2)

HAL is a multi-disciplinary open access archive for the deposit and dissemination of scientific research documents, whether they are published or not. The documents may come from teaching and research institutions in France or abroad, or from public or private research centers.

L'archive ouverte pluridisciplinaire **HAL**, est destinée au dépôt et à la diffusion de documents scientifiques de niveau recherche, publiés ou non, émanant des établissements d'enseignement et de recherche français ou étrangers, des laboratoires publics ou privés.

Matching of fundamental modes at a junction of a cylinder and a truncated cone; application to the calculation of radiation impedances

Jean Kergomard *

LMA, CNRS, UPR 7051, Aix-Marseille Univ, Centrale Marseille,
F-13402 Marseille Cedex 20, France

Antoine Lefebvre and Gary P. Scavone

Computational Acoustic Modeling Laboratory,
Centre for Interdisciplinary Research in Music Media and Technology (CIRMMT),
Schulich School of Music,
McGill University,
555 Sherbrooke Street West, Montréal, Québec H3A 1E3, Canada

March 23, 2015

Abstract

The problem of the junction between a cylinder and a truncated cone at low frequencies is investigated, in particular for the case of acute angles. An analytical model of the radiation impedance of the cylinder into the truncated cone is derived for the general case of a cone of finite length. When the cone is infinite and the angle is right, the problem is similar to the classical problem of a tube radiating in an infinite baffle. The model is based on a general formulation of the junction of several waveguides at low frequencies (when only the fundamental mode propagates in each guide), and on the assumption that at high frequencies, the radiation impedance of the cylinder is equal to its characteristic impedance. The model has the form of an equivalent circuit, and involves several parameters related to the geometry (the areas of the surfaces defining the matching cavity and the volume of this cavity). In addition, the model requires one supplementary parameter only, i.e., the low frequency value of the added mass (or length correction), which has to be determined numerically (the Finite Element Method is used). Analytical and numerical results agree very well at low and moderate frequencies, up to the cutoff of the first higher-order mode. For the radiation into an infinite flange, the results improve upon those in a recent publication that were obtained by optimization. The case of obtuse angles is more complicated and is briefly discussed. Finally for the case of infinite cones, the reflection coefficient is compared to that obtained in previous studies.

keywords: conical tubes, acoustic radiation impedance, cylinder-cone, wind instruments

*Tel 33 491164381, Fax 33 491228248, kergomard@lma.cnrs-mrs.fr

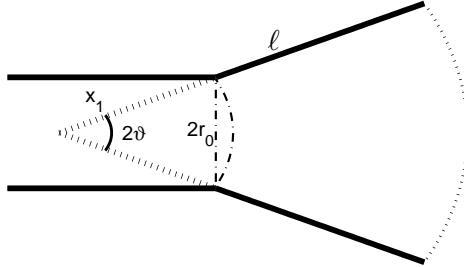


Figure 1: Geometry of the problem. The total length of the cone is $x_2 = \ell + x_1$, the half-angle at the apex is ϑ . The plane and spherical surfaces across the tubes define the junction of the two waveguides.

1 Introduction

The calculation of the radiation of tubes into infinite space, when only the fundamental, planar mode propagates, is a classical issue: the definitive papers are by Levine and Schwinger [1] for a tube without flange and Norris and Sheng [2] for a tube in an infinite flange. Conversely the more general problem of the radiation of a cylindrical tube into a conical tube has been rarely treated, but Chester [3] and Martin [4] gave interesting formulas for the case of small angles. The present paper investigates this problem, but generalizes it by considering the possibility of a finite length for the truncated cone. In other words, the matching of planar waves in a cylinder and spherical waves in a truncated cone is studied. Radiation will be a particular case when the cone is infinite. The basis of the study is a general formulation for the junction of several waveguides at low frequencies [5].

Figure 1 shows the geometry of the problem. Both tubes are without flow, and with perfectly rigid walls: thus the fundamental modes are uniform modes in both tubes. The subscript 0 refers to the output of the cylinder, while the subscripts 1 and 2 correspond to the input and output of the truncated cone. ϑ is the half-angle at the cone apex.

Section 2 describes the transfer matrix for the fundamental mode of spherical waves in a truncated cone. Section 3 presents the problem as a junction of two waveguides and the formulation as an equivalent electric circuit. Section 4 shows that this formulation, together with an assumption concerning the high frequency behavior, leads to a general approximate formula for the output impedance of the cylinder. With the knowledge of the geometry and only one supplementary parameter, which is the added mass at low frequencies, it is possible to deduce a complete impedance curve at frequencies lying below the cutoff of the first-order higher mode in the cylinder. This is the main result of the present paper. For the particular case of an infinite cone and an angle $\vartheta = \pi/2$, this formula is compared with the exact result given by Norris and

Sheng [2].

For other values of ϑ , no exact result is available. The Finite Element Method (FEM) is used for the case of cones of finite length, and this allows the added mass to be determined and then the comparison of the analytical formula with the numerical result. Section 6 presents the problem of obtuse angles. Finally, Section 7 presents the results of Chester [3] and Martin [4] in comparison with those given by the present method, for the case of an infinite cone.

2 Input admittance of a conical tube

Using a change in variables, the propagation of the fundamental mode of spherical waves can be classically described by a transfer matrix identical to that of planar waves (see e.g. [6]), as follows:

$$\begin{pmatrix} Px \\ \tilde{V}x \end{pmatrix}_1 = \begin{pmatrix} \cos k\ell & j\rho c \sin k\ell \\ j(\rho c)^{-1} \sin k\ell & \cos k\ell \end{pmatrix} \begin{pmatrix} Px \\ \tilde{V}x \end{pmatrix}_2 \quad (1)$$

with $\tilde{V}_i = V_i - \frac{P_i}{jk\rho c x_i} \quad i = 1, 2$

The equation is written in the frequency domain. P_i and V_i are the acoustic pressure and velocity at the distance x_i from the apex, $j^2 = -1$, c the speed of sound, ρ the gas density $k = \omega/c$, ω the angular frequency, $\ell = x_2 - x_1$. The quantity \tilde{V}_i can be called the symmetric velocity, because the asymmetric transmission line corresponding to spherical waves becomes symmetrical with this appropriate choice of variables. This allows a symmetric acoustic admittance, \tilde{Y}_i to be defined as:

$$\tilde{Y}_i = \frac{S_i \tilde{V}_i}{P_i} = Y_i - \frac{S_i}{j\omega\rho x_i} \quad (2)$$

where S_i is the cross section area at distance x_i from the apex. The expression of the area S_i of the spherical cap is $S_i = 2\pi x_i^2(1 - \cos \vartheta)$, with $\sin \vartheta = r_0/x_1$.

The fundamental mode is the only propagating mode up to the cutoff frequency of the first higher-order mode. In Ref. [7], an approximate formula is given for this frequency, which depends on the abscissa in the cone (thus on the radius r at this abscissa). We write it in the following form:

$$kr = \sqrt{\mu(\mu + 1)} \sin \vartheta \quad \text{with } \mu = \frac{3.832}{\vartheta(1 + 0.14\vartheta)}, \quad (3)$$

where μ is the order of the Legendre polynomial. When ϑ tends to 0 (case of a cylinder), kr tends to the well known value of 3.832 for a cylindrical tube. For ϑ increasing toward $\pi/2$, the value of kr decreases monotonically to $\sqrt{6} = 2.45$ ($\mu = 2$).

3 Matching of a cylinder and a truncated cone

In Ref. [5], a general low frequency formulation for the junction of several cylindrical guides was proposed. For the case where only one mode propagates, the

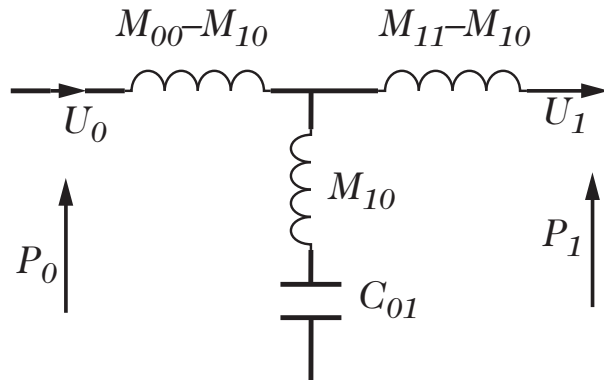


Figure 2: Equivalent electrical circuit of the junction between the two guides. The subscripts 0 and 1 correspond to the cylindrical and conical guides, respectively. $C_{01} = V/\rho c^2$, where V is the volume of the junction.

formulation takes into account the existence of evanescent modes in the different guides. When only two guides are considered (with indices 0 and 1), the formulation reduces to:

$$\begin{pmatrix} P_0 \\ P_1 \end{pmatrix} = \left[\frac{\rho c^2}{j\omega V} \begin{pmatrix} 1 & 1 \\ 1 & 1 \end{pmatrix} + j\omega \begin{pmatrix} M_{00} & M_{01} \\ M_{10} & M_{11} \end{pmatrix} + O(\omega^3) \right] \begin{pmatrix} U_0 \\ -U_1 \end{pmatrix} \quad (4)$$

$P_{0,1}$ and $U_{0,1}$ are the planar mode pressure and flow rate, respectively. The subscripts 0 and 1 are related to the surfaces defining the junction cavity: these surfaces can be chosen arbitrarily, but it is convenient to use a cavity as small as possible¹. The shape of the first matrix is due to the mass conservation (V is the volume of the junction). The minus sign before U_1 is used for convenience for ensuring the symmetry of the input and output, thus for exhibiting the symmetry of the matrix \mathbf{M} (which is due to reciprocity). \mathbf{M} is proportional to the density ρ . The elements M_{ij} , which represent the effect of evanescent modes on both sides of the junction, can be calculated by solving the Laplace equation (for an incompressible fluid). The terms of higher order in frequency are matrices depending on both the compressibility and the density. Equivalently, they can be replaced by a variation of the elements of the matrix \mathbf{M} with frequency. The equivalent electrical circuit is shown in Fig. 2.

The derivation of Eq. (4) is detailed in Ref. [5]. The result is formal, because the method is in general not an effective computation method of the elements of the matrices. It is based on several steps: i) derivation of an integral equation for the matching cavity with the free space Green function; ii) projection on the modes of the different guides; iii) closing of the evanescent modes on their characteristic impedance (a condition of validity of Eq. (4) is that the length of each guide is long enough and avoids any coupling of the extremities by evanescent modes); and finally iv) a series expansion of the Green function with respect to frequency.

¹For certain cases, it is possible to choose a junction without volume (e.g., for a sudden discontinuity in cross section). Then the equations are replaced by $U_0 + U_1 = 0$, and the expression of $P_0 - P_1$ with respect to the flow rates.

This formulation is valid also for the fundamental mode of spherical waves, when it is the unique propagating mode, and can be used for the junction between a cylindrical guide of radius r_0 , and a truncated cone. The matching volume between the output of the cylinder and the input of the truncated cone (see Fig. 1) has the following expression:

$$V = \pi r_0^3 \frac{\sin \vartheta [2 + \cos \vartheta]}{3 [1 + \cos \vartheta]^2}. \quad (5)$$

It is convenient to reduce the problem by using dimensionless variables: the impedances are reduced by the characteristic impedance of the cylindrical tube, $Z_{c0} = \rho c / (\pi r_0^2)$. Lowercase characters are used for the dimensionless variables (e.g. y_1 is the dimensionless version of Y_1 in Eq. (2)). kr_0 is the reduced frequency, and the Laplace variable is noted $s = jkr_0$. The following expressions are found:

$$y_1 = \tilde{y}_1 + \frac{1}{sm_1}, \text{ with } m_1 = \frac{\zeta}{\sin \vartheta}; \quad \zeta = \frac{1 + \cos \vartheta}{2}; \quad (6)$$

$$j\omega \frac{V}{\rho c^2} \frac{\rho c}{\pi r_1^2} = sc_{01} \text{ with } c_{01} = \frac{V}{\pi r_0^3}; \quad (7)$$

$$j\omega M_{ij} \frac{\pi r_1^2}{\rho c} = sm_{ij}, \text{ where } m_{ij} = M_{ij} \frac{\pi r_0}{\rho} \quad (8)$$

ζ is the ratio of plane to spherical surfaces. The output impedance $z_0 = P_0/U_0$ of the cylindrical tube is given by Eq. (4), or by the equivalent circuit of Fig. 2. After some algebra, it is found to be:

$$z_0 = \frac{\left[\frac{1}{y_1} + sm_{11} - sm_{10} \right] \left[\frac{1}{sc_{01}} + sm_{10} \right]}{\left[\frac{1}{sc_{01}} + \frac{1}{y_1} + sm_{11} \right]} + s(m_{00} - m_{10}). \quad (9)$$

4 General formulas for the output impedance of the cylinder

4.1 Conditions for the case of an infinite conical tube

Consider an infinite conical tube. It is assumed that for any value of ϑ , the high-frequency asymptotic value of a radiation impedance z_0 is the characteristic impedance Z_{c0} of the fundamental mode in the cone. Relationships between the masses m_{ij} are sought by using this assumption. At the input of the truncated cone, the symmetric admittance is $\tilde{Y}_1 = S_1/\rho c$, thus:

$$y_1 = \frac{1}{\zeta} + \frac{1}{sm_1} = \frac{1}{\zeta} \left[1 + \frac{\sin \vartheta}{s} \right]. \quad (10)$$

At higher frequencies, the compliance term $1/(sc_{01})$ is of order s^{-1} , and can be neglected in Eq. (9). Similarly $1/y_1 \simeq \zeta$. Thus at higher frequencies:

$$z_0 \simeq \frac{-s^2 m_{10}^2}{\zeta + sm_{11}} + sm_{00} = 1. \quad (11)$$

The identification of the two highest order terms leads to:

$$m_{10}^2 = m_{11}m_{00} \quad (12)$$

$$m_{11} = \zeta m_{00}. \quad (13)$$

Eq. (12) gives two solutions for m_{10} . The positive value leads to a resonant curve for the output impedance, while the negative value gives a very good approximation formula, as shown hereafter.

At lower frequencies: z_0 reduces to the impedance of a mass, and is denoted sm :

$$z_0 = sm = s(m_1 + m_{11} - 2m_{10} + m_{00}). \quad (14)$$

m needs to be computed by numerical methods (which is done in Section 5). It is the coefficient of the so-called “length correction” at the end of the cylindrical tube, or more accurately, the added mass. For the limit case $\vartheta = \pi/2$ (tube in an infinite baffle), it is known to be $m = 0.82159$ (see [2,8]). With the knowledge of this quantity, the model is complete. The three masses m_{ij} are given by:

$$m_{00} = (m - m_1)/(1 + \sqrt{\zeta})^2; \quad (15)$$

$$m_{11} = \zeta m_{00}; m_{10} = -\sqrt{\zeta} m_{00}.$$

4.2 General and simplified formulas

The general formula is therefore as follows:

$$z_0 = \frac{1 + y_1 s(m - m_1) + s^2 c_{01} m_{00}}{s c_{01} + y_1 (1 + s^2 c_{01} m_{11})}. \quad (16)$$

For the case of an infinite cone, this formula becomes:

$$z_0 = \frac{sm + s^2(m - m_1)m_1/\zeta + s^3 m_1 c_{01} m_{00}}{1 + sm_1/\zeta + s^2 c_{01}(m_{11} + m_1) + s^3 m_1 c_{01} m_{00}}. \quad (17)$$

At lower frequencies, it can be checked that:

$$Re(z_0) = -s^2 m_1^2 / \zeta = Re(1/y_1). \quad (18)$$

This is due to the conservation of both the acoustic power and the flow rate between the two surfaces S_0 and S_1 .

In Section 5 it will be shown that $m - m_1 \approx \zeta c_{01}$. Thus a simplified expression can be sought for Eq. (16), in particular for smaller angles and lower frequencies:

$$z_0 = \frac{1 + y_1 s c_{01} \zeta}{s c_{01} + y_1}. \quad (19)$$

4.3 Case of the radiation into an infinite flange

For the case $\vartheta = \pi/2$, Eq. (17) becomes:

$$z_0 = \frac{0.82159s + 0.3216s^2 + 0.0368s^3}{1 + s + 0.3701s^2 + 0.0368s^3}, \quad (20)$$

For this case, looking at the poles of the denominator, it can be checked that two roots are complex conjugate and one is real, all real parts being negative.

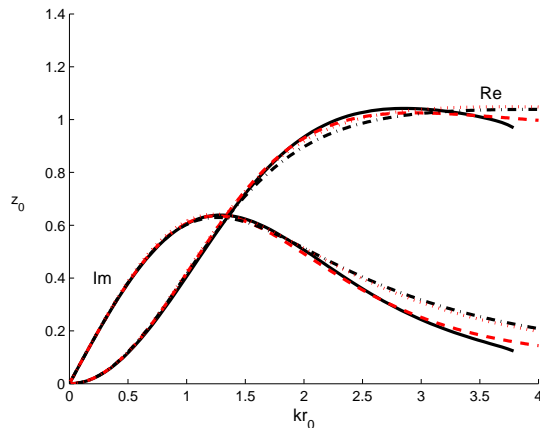


Figure 3: Real and imaginary parts of the radiation impedance z_0 in an infinite flange ($\vartheta = 90$). Black, solid line: exact result [2]; black, dash-dot line, approximate result [9]; grey (red online), dashed line: Eq. (20); grey (red online), dotted line: Eq. (21).

Thus the inverse Fourier Transform is causal (see Ref. [9]). Figure 3 shows the comparison of the exact result (Ref. [2]) with the approximate formula given in Ref. [9], and with Eq. (20). Except at very high frequencies, this formula is excellent. This is remarkable, because it is built with the knowledge of the low frequency added mass only. As explained in Section 2, the expected limit of validity of Eq. (20) is $kr_0 = 2.45$. However the equation remains valid for frequencies above this limit, where at least two propagating modes are expected, as well as a corresponding directivity pattern in the radiated field.

For the same case, $c_{01} = 2/3$, and Eq. (19) becomes:

$$z_0 = \frac{5s/6 + s^2/3}{1 + s + s^2/3}. \quad (21)$$

The simplicity of this formula is remarkable. $5/6 = 0.8333$ is very close to the exact value of the length correction at zero frequency. The other coefficients are close to those obtained by optimization in [9]: 0.324 instead of $1/3$ and 1.003 instead of 1 (for the term in s) in the denominator. Figure 3 shows that the result of Eq. (21) is very close to that of Ref. [9].

5 Numerical calculation of the low frequency added mass

5.1 Method

For $\vartheta < \pi/2$, the added mass coefficient m is not known. Therefore a numerical method, the FEM is used. In order to avoid complications with an anechoic termination, two reactive boundary conditions are investigated: i) a rigid wall; and ii) a perfectly soft wall. In both cases the wall is perfectly spherical and

the condition is valid at every angle, thus at the input of the cone, ideally only the fundamental mode can be propagating under the cutoff of the higher-order modes. The cylinder has a certain length, ℓ_0 , sufficient to avoid the presence of evanescent modes at its input. The computed input impedance of the cylinder is projected to its output, giving the desired impedance z_0 , and the mass m is obtained by using formula (16) at low frequency.

The FE model was formed as an axi-symmetric geometry. The cylinder radius and length were 1 and 5 cm, respectively, and the truncated conic section was 5 cm long, as measured along its central axis, for all cone half angles. The side walls were defined as rigid and the spherical boundary at the output of the cone was defined as either rigid or soft ($P_2 = 0$). A constant acceleration was specified across the entire input plane. A fine mesh was constructed with triangular elements and a maximum element size of 0.001 meter. Numerical simulations were conducted for cone half angles from 5 to 105 degrees in increments of 5 degrees, with an additional set of simulations at 115, 125, and 135 degrees.

5.2 Numerical result for the low frequency added mass

From the knowledge of the admittance at the output of the cone, Y_2 , the input admittance y_1 is derived. Using Eqs. (1) and (6), the following expression is found:

$$y_1 = \frac{1}{sm_1} + \frac{1}{\zeta} \frac{j \tan k\ell + \tilde{Y}_2 \rho c / S_2}{1 + j \tilde{Y}_2 \rho c / S_2 \tan k\ell}. \quad (22)$$

For a perfectly soft termination ($Y_2 = \infty$), \tilde{Y}_2 is infinite, while for a perfectly rigid termination, $\tilde{Y}_2 \rho c / S_2 = -1/(jkx_2)$. In both cases, the admittance y_1 is purely imaginary. The value of the mass m is derived from Eq. (16):

$$m = m_1 + \frac{z_0(y_1 + sc_{01}) - 1}{s [y_1 + sc_{01}(1 - \zeta z_0 y_1)/(1 + \sqrt{\zeta})^2]}. \quad (23)$$

For $kr_0 = 0.01$, the accuracy of the value of m can be assessed to be better than 0.1%, when changing the frequency to another low frequency, or when changing the termination (soft to rigid), or when changing the length ℓ of the truncated cone. The calculation is done for several values ϑ . Figure 4 shows that the mass $m - m_1$ is roughly proportional to the quantity ζc_{01} , the ratio ranging between 0.93 and unity. A fit formula is found to be:

$$m - m_1 \simeq \zeta c_{01} [1 - 0.075 \sin(1.75 * \vartheta)] \quad (24)$$

with an error smaller than 1% for $\vartheta < \pi/2$. For small angles, $\zeta c_{01} \ll m_1$. This leads to the simplest value for m : $m = m_1 = 0.5 \cot(\vartheta/2)$. The latter expression is equivalent to that of Tyte [10].

5.3 Verification for the case of cones of finite length

With the value obtained for the mass m , it is possible to compare the general model (16) with the FEM result for a cone of finite length, for the two terminations considered. The model is found to be very good, as shown in Figs. 5 and 8 for the case $\vartheta = 50$. For this angle, the cutoff frequency of the first higher order mode at the cone input is $kr_0 = 3.36$. Figure 6 shows the pressure field

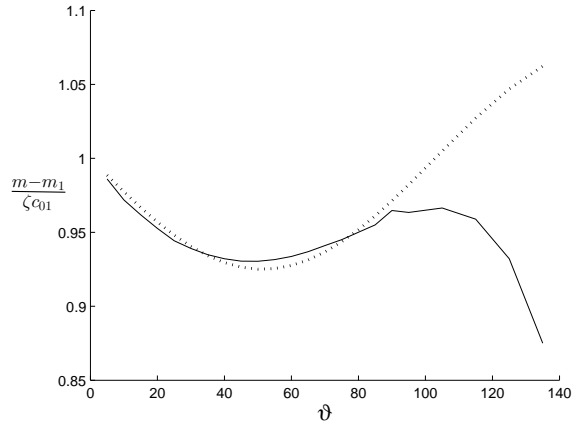


Figure 4: The quantity $(m - m_1)/\zeta c_{10}$ with respect to the angle ϑ (in degrees). Dotted line: expression given by Eq. (24).

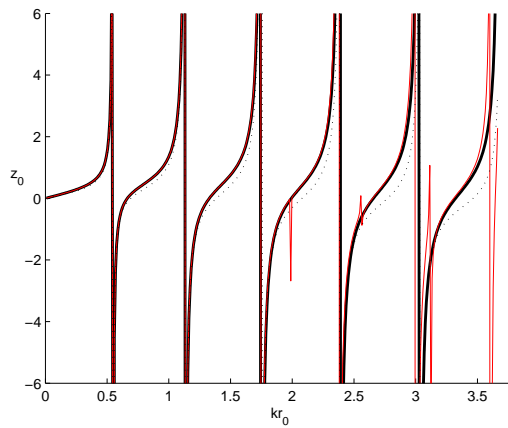


Figure 5: Output impedance z_0 (imaginary part) of a cylinder terminated in a truncated cone, the latter being terminated into a perfectly soft spherical cap. $\vartheta = 50$. FEM result: grey (red online) line; Formula (16): black, solid line; Formula (19): dotted line. At low frequencies, the FEM results and Eq. (16) are indistinguishable. Above middle frequencies, non-axisymmetric modes appear in the FEM curve.

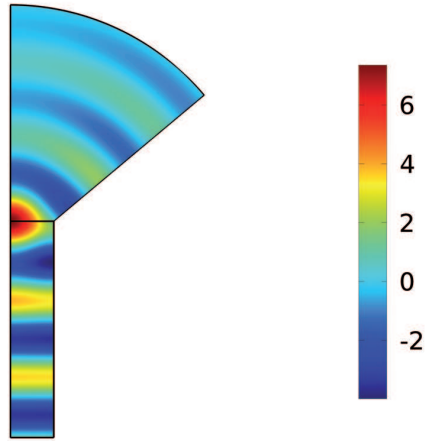


Figure 6: Pressure field for a frequency above the first cutoff frequency: $kr_0 = 3.57$. $\vartheta = 50$. One half of the system is shown. The scale is arbitrary.

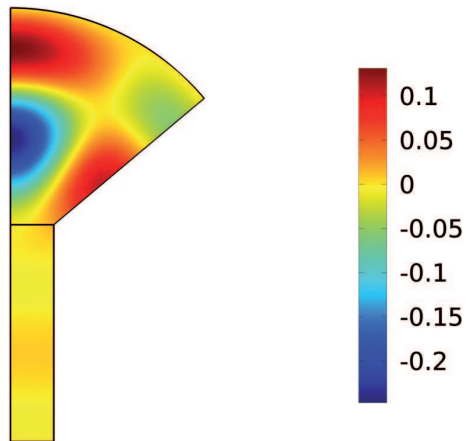


Figure 7: Pressure field for a frequency corresponding to a non axi-symmetric mode. $kr_0 = 1.99$. $\vartheta = 50$. One half of the system is shown. The scale is arbitrary.

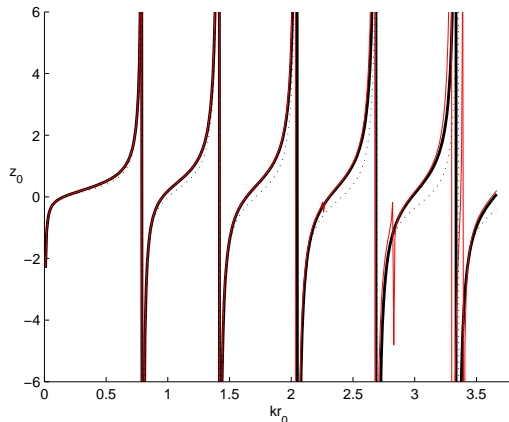


Figure 8: Output impedance z_0 (imaginary part) of a cylinder terminated in a truncated cone, the latter being terminated into a perfectly rigid spherical cap. $\vartheta = 50$. FEM result: grey (red online) line; Formula (16): black line; Formula (19): dotted line. At low frequencies, the FEM results and Eq. (16) are indistinguishable. Above middle frequencies, non-axisymmetric modes appear in the FEM curve.

for a frequency higher than the cutoff ($kr_0 = 3.57$). A slight dependence of the field on the angle ϑ is observed.

At rather high frequencies, the FEM results exhibit thin peaks on the output impedance curve: these peaks do not exist in the analytical formula. The reason lies in the creation of higher order spherical, propagating modes. The above mentioned cutoff value $kr_0 = 3.57$ corresponds to the property of the modes at the entry of the truncated cone. However, the duct modes which are evanescent at this location are propagating far from the entry. For the example computed, the cutoff at the output of the truncated cone is 4.47 times lower. Therefore a kind of tunneling effect can happen, and cavity modes (i.e., modes of a cone of finite length) can be created (by the change in conicity) without spherical symmetry through evanescent duct modes. It has been checked that for certain frequencies, the spherical symmetry is destroyed in the cone, and nodal lines appear: this is shown in Fig. 7 for the frequency of the first non-axisymmetric mode in Fig. 5, at $kr_0 = 1.99$. This mode shape is similar to those found in the work by Hoersch [11].

Going further in the comparison between numerical results and the formulas, we choose to compute the relative error for the first and second impedance minima (anti-resonances), defined as follows: $error = (f_a/f_b - 1)$, where f_a and f_b are the analytical and numerical results, respectively. The relative error for the resonance frequencies is less useful because it is extremely small, and the calculation of an average error on the impedance value over the frequency range would be more difficult to interpret. Figure 9 shows that the error increases monotonically when the angle ϑ increases. Results for the two formulas (16) and (19) can also be distinguished. The results for an intermediate formula, obtained by using the value of m given by Eq. (24) into Eq. (16) are not shown, because they are very close to those of Eq. (16) with the numerical value of m .

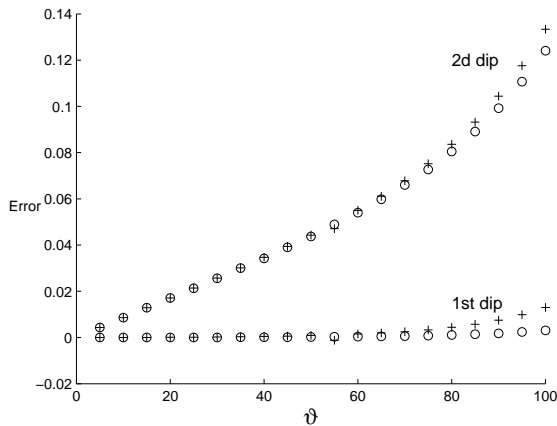


Figure 9: Relative error for the frequencies of the first and second minima of impedance modulus $|z_0|$ (ϑ in degrees) ooo Eq. (16), +++ Eq. (19). The termination of the cone is perfectly soft.

Figure 9 shows also some results for obtuse angles, which are discussed in the next section.

6 The case of obtuse angles

6.1 Limit of the extension of the previous analysis

When the angle ϑ is obtuse, the distance between the plane and spherical surfaces of the matching volume becomes large, and it cannot be regarded as smaller than the wavelength. Therefore it is expected that the results become much less accurate for such angles. However it is observed in Fig. 9 that up to $\vartheta = 100^\circ$, there is a perfect continuity of the error, and the analytical formulas remain satisfactory. Then, above this value, the error rapidly increases. Therefore another model should be found for a correct description of this case. A recent paper investigated this case using a hybrid FEM [12].

6.2 Radiation of cylindrical tube without flange

For the case $\vartheta = \pi$, the results are expected to be very bad, because many coefficients of the formula diverge (this case corresponds to the radiation of a tube without flange, see Ref [1]). The limit of formula (17) is undetermined, and its use is meaningless, because the apex of the cone tends to infinity and therefore the radius x_1 becomes infinite.

However another model can be considered, with a sphere having *its center at the output of the cylinder*, and with a radius R . The same calculations as previously described can be made with the following parameters:

$$\zeta = \frac{\alpha^2}{4} ; m_1 = \frac{\alpha}{4} ; c_{10} = \frac{4}{\alpha^3} \quad (25)$$

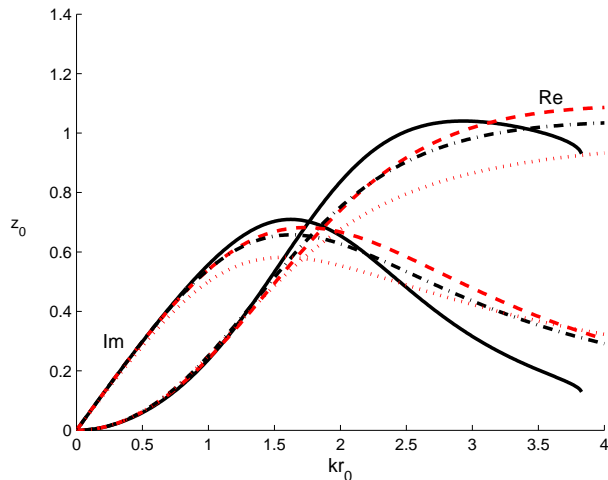


Figure 10: Real and imaginary parts of the radiation impedance z_0 without flange ($\vartheta = 180$). Black, solid line: exact result [1]; black, dash-dot line, approximate result [9]; grey (red online), dashed line: Eq. (17) for $\alpha = 1$; grey (red online), dotted line: Eq. (26).

where $\alpha = r_0/R$. With the knowledge of the added-mass coefficient $m = 0.6133$, Eq. (17) can be used. Empirically it is found that the best value for R is close to r_0 . We have not yet a clear interpretation of this result. Figure 10 shows the comparison of the exact result of Ref. [1] with that of Eq. (17) for $\alpha = 1$ and with the result proposed by Ref. [9]. The accuracy of the two approximate results is similar, but the qualitative conclusion of the present paper remains valid: with the knowledge of the low frequency added mass, it is possible to deduce a rather satisfactory approximate impedance curve.

Furthermore, the simplified formula (19) leads to the following result:

$$z_0 = \frac{7s/12 + s^2/3}{1 + s + s^2/3} \quad (26)$$

where $7/12 = 0.5833$. A discussion similar to that provided for the infinite flange case can be applied, but this formula is less satisfactory than Eq. (21) (see Fig. 10).

7 Small angles; discussion of previous results of the literature for the case of an infinite cone

The present section aims to discuss the results of Chester [3] and Martin [4] concerning the case of an infinite cone. The comparison will be done for the modulus of the reflection coefficient of planar waves in the cylindrical duct (for brevity we do not discuss the behavior of the argument).

Chester gave an analytical formula, obtained with the following hypothesis: the expansion in modes of the cylindrical duct can be extended inside the

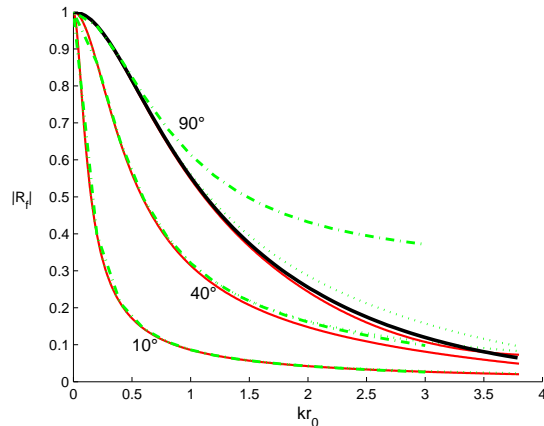


Figure 11: Modulus of the reflection coefficient at the output of the cylinder for three angles: 10, 40 and 90 degrees. Comparison of Martin's formula (dotted line, green online) and Chester's formula (dash-dot line, green online) with Eq. (16) (solid line, red online). The black, thick line is the exact result for 90 degrees.

matching volume (notice that this implies that the rigid walls of the cylinder are elongated). Eqs. (15) and (4) of Chester's paper give the value of the impedance z_0 . Numerical coefficients are given by a table. We do not reproduce the data here, but Fig. 11 shows the result, and compares it to Formulas (16) and (19), with $R_f = (z_0 - 1)/(z_0 + 1)$, for 3 values of ϑ and with the exact result for $\vartheta = 90$. Chester's formula appears to be useful only at rather small angles. It can be noticed that the author himself mentioned that for smaller angles the result is very close to that of a simplified formula, which it turns out is that $z_0 = 1/y_1$ (with the addition of a phase shift).

In Ref. [4], Martin gave another approximate formula. The method was the analytical application of the Green theorem, and the expected validity is for small angles and low frequencies. The formula can be written in the form:

$$R_f = \frac{\sin^2 \vartheta - 4\zeta [\exp(-s \sin(\vartheta)/(2\zeta)) - 1]}{-\sin^2 \vartheta + 4\zeta s^2}. \quad (27)$$

Figure 11 shows that it is an excellent approximation for small angles, and it is less satisfactory for wide angles.

Furthermore Martin discussed simplified formulas for small angles and low frequencies. He gave an expansion with respect to frequency, limited to the first order of the frequency. This yields $R_f = -1 + 2s \csc \vartheta$, and a negative real part of the impedance z_0 . However if the orders of magnitude of ϑ and s are considered to be similar, the following formula is found:

$$R_f = -\frac{\vartheta}{\vartheta + 2s}. \quad (28)$$

This result is the same by using either Formula (19) or Formula (27), the missing terms being of the 3rd order ($s\vartheta^2$, ϑs^2). This corresponds to Eq. (6) for

small angles, therefore to the assumption that both the mass ($m - m_1$) and the matching volume can be ignored. This approximation is consistent with the approximation of the horn equation (often called "Webster equation") written in spherical waves (see [7, 13]), which leads to an accuracy much higher than that using plane waves [14].

8 Conclusion

The main interest of the approach presented in the paper is the possibility to derive a knowledge of a complete impedance curve from the knowledge of the geometry and one supplementary parameter only: the low frequency added mass. Formula (16) together with the fit formula (24) gives very satisfactory results when compared to numerical results for finite length cones and acute angles.

The case of obtuse angles seems to be more difficult, even if the results for slightly obtuse angles are not bad. The limitation is not only relative to angles, but also to frequencies: this is not surprising, and anyway in practice, for non perfectly cylindrical tubes, the appearance of higher order propagating modes occurs near $kr_0 = 1.8$.

The results for the standard case of the radiation of a tube without flange or with an infinite flange compare favorably with the fit formulas obtained by optimization in Ref. [9].

It is remarkable that approximate formulas can take various forms (see Refs. [3, 4, 9]). Our formulation derives from an electrical circuit. Would it be possible to improve it? Three new parameters would be added if the third-order terms in Eq. (4) are included. This would likely be possible, but in practice, situations at higher frequencies with one propagating mode only are rare.

Finally, it is probable that the use of the general formulation (4) could be used also for other problems, such as the matching of truncated cones with different angles.

References

- [1] H. Levine and J. Schwinger, On the radiation of sound from an unflanged circular pipe. *Phys. Rev.* 73 (1948), 383-406.
- [2] A.N.Norris, I.C. Sheng, Acoustic radiation from a circular pipe with an infinite flange. *J. Sound Vib.* 135 (1989) 85-93.
- [3] W. Chester, The acoustic impedance of a semi-infinite tube fitted with a conical flange: Part II. *J. Sound Vib.* 116 (1987) 371-377.
- [4] P.A. Martin, The horn-feed problem: sound waves in a tube joined to a cone, and related problems. *J. Eng. Math.* 71 (2011) 291-304.
- [5] J. Kergomard, A. Khettabi, A. Garcia, General formulation of waveguide junction at low frequencies, *C.R. Acad. Sci., Paris*, t. 319, II, (1994), 887-892.

- [6] R. Caussé, J. Kergomard, X. Lurton, Input impedance of brass musical instruments: comparison between experiment and numerical models. *J. Acoust. Soc. Am.* 75 (1984) 241-254.
- [7] A.H. Benade and E.V. Jansson. On plane and spherical waves in horns with nonuniform area. *Acustica*, 31 (1974) 80-98.
- [8] L. V. King, On the electrical and acoustic conductivities of cylindrical tubes bounded by infinite flanges. *Phil. Mag.* 21 (1936), 128-144.
- [9] F. Silva, Guillemain, P., Kergomard, J., Mallaroni, B., Norris, A., Approximation of the acoustic radiation impedance of a cylindrical pipe. *J. Sound Vib.*, 322 (2009), 255-263.
- [10] L.C. Tyte, Some notes on end-corrections, *Phil. Mag.* 7, 30 (1940), 173-184.
- [11] V.A. Hoersch, Non-radial harmonic vibrations within a conical horn, *Phys. Rev.* 25 (1925), 218-224.
- [12] W. Duan and R. Kirby, A hybrid finite element approach to modeling sound radiation from circular and rectangular ducts, *J. Acoust. Soc. Am.*, 131 (2012), 3638-3649.
- [13] T. Hélie. Unidimensional models of acoustic propagation in axisymmetric waveguides. *J. Acoust. Soc. Am.*, 114 (2003) 2633-2647.
- [14] T. Hélie, T. Hézard, R. Mignot, D. Matignon, One-Dimensional Acoustic Models of Horns and Comparison with Measurements. *Acta Acustica united with Acustica*, 99 (2013) 960 – 974.